Journal of Organometallic Chemistry, 331 (1987) 263–270
Elsevier Sequoia S.A., Lausanne – Printed in The Netherlands

Structural study of bis(η-cyclopentadienyl)dicarbonyliron (p-tolyl)tin(IV) bromide

Zu-Tao Wang

Tianjin Advanced Institute of Science and Technology, Tianjin (China)

Hsu-Kun Wang*, Xiang-Yang Liu, Xing-Kai Yao, and Hung-Gen Wang

Institute of Elementoorganic Chemistry, Center of Measurement and Computation,
Nankai University, Tianjin (China)

(Received December 10th, 1986; in revised form March 5th, 1987)

Abstract

The compound, $[\eta\text{-}C_5H_5Fe(CO)_2]_2(p\text{-}CH_3C_6H_4)SnBr$, crystallizes in the monoclinic space group $P2_1/c$ with a 9.643, b 12.016, c 19.205 Å, β 98.68°, V 2225.9 Å^3, and $Z = 4$. The crystal and molecular structures have been solved by use of the Patterson method. A full-matrix least-squares refinement led to a final R value of 0.036 for 3260 independent observed reflections. The electronic structure was calculated by use of the EHMO quantum chemical method. The molecular features and the influence on the coordinate geometry, and the nature of the bonding of the central tin atom are discussed.

Introduction

A number of metal cluster compounds containing tin and iron bonds have been studied [1–8]. The most unusual feature of these molecules is that the bond distances and bond angles vary with the coordination environment of the tin atom. We recently synthesized a new compound, $[\eta\text{-}C_5H_5Fe(CO)_2]_2Sn(p\text{-}CH_3C_6H_4)Br$, and characterized it [9]. The crystal structure was determined and an EHMO calculation was carried out to interpret the coordination geometry and the nature of the bonding around the central tin atom.

X-ray diffraction study

The pale red, polyhedral single crystal of $[\eta\text{-}C_5H_5Fe(CO)_2]_2Sn(p\text{-}CH_3C_6H_4)Br$ was obtained on recrystallization from a mixed solvent (acetone/methanol). A crystal with approximate dimensions 0.2 × 0.3 × 0.3 mm, was mounted on a glass

0022-328X/87/$03.50

Table 1

Crystal data of $[\eta\text{-}C_5H_5Fe(CO)_2]_2Sn(p\text{-}CH_3C_6H_4)Br$

Formula	$C_{21}H_{17}BrFe_2O_4Sn$	d_{calc} (g cm^{-3})	1.943
MW	643.547	Space group	Monoclinic: C_{2h}^5-$P2_1/c$
a (Å)	9.643(1)	Scan mode	$\omega/2\theta$
b (Å)	12.016(2)	Radiation	Mo-K_α
c (Å)	19.205(4)	θ_{max} (°)	25
β (°)	98.68(1)	No. of unique reflections	3260
V(Å^3)	2225.3	R	0.036
Z	4	R_w	0.046

fiber in an arbitrary orientation. Preliminary examination and data collection were performed with Mo-K_α radiation (λ 0.71073 Å) on an Enraf–Nonius CAD-4 computer-controlled kappa-axis diffractometer equipped with a graphite monochromator.

Cell constants and an orientation matrix for data collection were obtained from

Table 2

Fractional atomic coordinates and B_{eq} values for non-hydrogen atoms for $[\eta\text{-}C_5H_5Fe(CO)_2]_2Sn(p\text{-}CH_3C_6H_4)Br$

Atom	x	y	z	B_{eq} (Å^2)
Sn	0.22339(5)	0.26244(4)	0.66252(3)	2.448(8)
Br	0.2178(1)	0.46954(8)	0.69609(6)	5.41(2)
Fe(1)	0.4564(1)	0.2685(1)	0.11864(6)	3.03(2)
Fe(2)	0.1564(1)	0.3366(1)	0.22921(6)	3.15(2)
C(11)	0.408(1)	0.395(1)	0.0449(6)	7.3(3)
C(12)	0.544(1)	0.375(1)	0.0425(6)	9.3(3)
C(13)	0.377(1)	0.628(1)	0.8950(8)	10.0(4)
C(14)	0.462(2)	0.5759(9)	0.8519(6)	9.4(3)
C(15)	0.407(1)	0.4377(8)	0.1095(7)	7.5(3)
C(111)	0.4627(8)	0.6902(7)	0.3083(5)	3.9(2)
C(111)	0.4100(6)	0.6386(6)	0.2628(4)	5.8(2)
C(112)	0.4143(9)	0.3507(8)	0.5666(5)	4.7(2)
C(112)	0.3914(9)	0.4277(7)	0.5319(4)	7.5(2)
C(21)	0.153(1)	0.348(1)	0.3777(5)	5.5(2)
C(22)	0.202(1)	0.239(1)	0.3601(5)	5.2(2)
C(23)	0.3289(9)	0.256(1)	0.3296(4)	5.0(2)
C(24)	0.3533(9)	0.372(1)	0.3279(5)	5.2(2)
C(25)	0.246(1)	0.428(1)	0.3584(5)	5.6(2)
C(221)	0.1167(9)	0.4554(8)	0.2162(5)	4.2(2)
C(221)	0.0923(9)	0.5320(6)	0.1823(4)	6.6(2)
C(222)	0.0128(9)	0.7812(8)	0.2469(5)	4.3(2)
C(222)	0.1224(6)	0.7474(8)	0.2734(4)	6.8(2)
C(31)	0.0518(7)	0.2649(6)	0.5748(4)	2.8(1)
C(32)	0.0232(9)	0.6397(7)	0.4463(5)	4.2(2)
C(33)	0.1323(9)	0.6414(8)	0.5034(5)	4.5(2)
C(34)	0.1663(8)	0.7372(7)	0.5406(4)	3.4(2)
C(35)	0.0913(9)	0.6673(7)	0.0212(5)	4.1(2)
C(36)	0.9830(9)	0.6680(7)	0.9637(5)	4.0(2)
C(37)	0.2835(9)	0.7617(9)	0.1031(5)	5.3(2)

Table 3

Bond distances (Å) for $[\eta\text{-}C_5H_5Fe(CO)_2]_2Sn(p\text{-}CH_3C_6H_4)Br$

Sn–Br	2.573(1)	C(21)–C(22)	1.448(9)
Sn–Fe(1)	2.543(1)	C(22)–C(23)	1.450(8)
Sn–Fe(2)	2.536(1)	C(23)–C(24)	1.420(9)
Sn–C(31)	2.177(4)	C(24)–C(25)	1.430(8)
Fe(1)–C(111)	1.770(6)	C(25)–C(21)	1.408(9)
Fe(1)–C(112)	1.758(6)	C(221)–O(221)	1.132(6)
C(11)–C(12)	1.396(11)	C(222)–O(222)	1.132(6)
C(12)–C(13)	1.332(13)	C(31)–C(32)	1.383(6)
C(13)–C(14)	1.397(14)	C(32)–C(33)	1.401(7)
C(14)–C(15)	1.375(13)	C(33)–C(34)	1.369(7)
C(15)–C(11)	1.344(11)	C(34)–C(35)	1.378(7)
C(111)–O(111)	1.127(6)	C(35)–C(36)	1.401(6)
C(112)–O(112)	1.142(7)	C(36)–C(31)	1.393(6)
Fe(2)–C(221)	1.761(6)	C(34)–C(37)	1.519(6)
Fe(2)–C(222)	1.763(5)		

least-squares refinement of 25 reflections from the setting angles measured by use of the computer-controlled diagonal slit method of centering. The data were collected at room temperature by using the $\omega/2\theta$ scan technique. A total of 4195 reflections in the range of $2° \leqslant \theta \leqslant 25°$ were collected. After the Lorentz and polarization corrections had been applied, absorption was corrected for by an empirical method [10]. The cell parameters and conditions for data collection are listed in Table 1.

Table 4

Bond angles (°) for $[\eta\text{-}C_5H_5Fe(CO)_2]_2Sn(p\text{-}CH_3C_6H_4)Br$

Br–Sn–Fe(1)	106.09(2)	Sn–Fe(2)–C(221)	88.4(2)
Br–Sn–Fe(2)	103.52(2)	Sn–Fe(2)–C(222)	86.0(2)
Br–Sn–C(31)	98.0(1)	C(221)–Fe(2)–C(222)	91.8(3)
Fe(1)–Sn–Fe(2)	123.01(2)	Sn–Fe(2)–C(21)	151.6(2)
Fe(2)–Sn–C(31)	112.0(1)	Sn–Fe(2)–C(22)	111.4(2)
Fe(1)–Sn–C(31)	110.6(1)	Sn–Fe(2)–C(23)	87.3(2)
Sn–Fe(1)–C(111)	88.0(2)	Sn–Fe(2)–C(24)	102.1(2)
Sn–Fe(1)–C(112)	86.0(2)	Sn–Fe(2)–C(25)	141.0(2)
C(111)–Fe(1)–C(112)	93.1(3)	Fe(2)–C(221)–O(221)	179.5(5)
Sn–Fe(1)–C(11)	102.4(3)	Fe(2)–C(222)–O(222)	178.8(6)
Sn–Fe(1)–C(12)	141.1(4)	C(21)–C(22)–C(23)	107.1(6)
Sn–Fe(1)–C(13)	150.0(4)	C(22)–C(23)–C(24)	107.5(6)
Sn–Fe(1)–C(14)	111.0(4)	C(23)–C(24)–C(25)	108.7(6)
Sn–Fe(1)–C(15)	88.1(2)	C(24)–C(25)–C(21)	108.4(6)
Fe(1)–C(111)–O(111)	178.4(5)	C(25)–C(21)–C(22)	108.2(5)
Fe(1)–C(112)–O(112)	177.6(5)	C(31)–C(32)–C(33)	120.9(5)
C(11)–C(12)–C(13)	109.5(8)	C(32)–C(33)–C(34)	121.0(5)
C(12)–C(13)–C(14)	106.9(8)	C(33)–C(34)–C(35)	119.0(4)
C(13)–C(14)–C(15)	107.9(8)	C(34)–C(35)–C(36)	120.5(5)
C(14)–C(15)–C(11)	108.4(8)	C(35)–C(36)–C(31)	120.9(4)
C(15)–C(11)–C(12)	107.3(8)	C(36)–C(31)–C(32)	117.7(4)
Sn–C(31)–C(32)	122.7(3)	C(35)–C(34)–C(37)	120.3(5)
Sn–C(31)–C(36)	119.5(3)	C(33)–C(34)–C(37)	120.8(5)

The structure was solved by direct methods. The positions of Sn and Fe were found from the E-map. The coordinates of non-hydrogen atoms were obtained through several difference-Fourier syntheses. Only the 3260 reflections with intensities greater than 3.0σ were used in the refinement. The final unweighted and weighted R factors were 0.036 and 0.046, respectively.

All calculations were carried out on a PDP-11 computer with SDP-PLUS [11].

Fractional atomic coordinates and equivalent isotropic thermal parameters for the non-hydrogen atoms are given in Table 2. The bond distances and bond angles are given in Tables 3 and 4, respectively.

Quantum chemical calculation

The computation was carried out with the EHMO program [12] on an M160 computer. The atomic coordinates of non-hydrogen atoms were taken from our crystal structure analysis and the coordinates of hydrogen atoms were calculated in accordance with standard C–H bond distances and angles. In addition, the crystallographic origin of coordinates was transferred to the tin position, the Sn–Fe(1) axis was assigned as the x axis, and Sn–Fe(1)–Fe(2) plane was chosen as xy plane. The parameters used in this EHMO calculation are listed below:

Atom	Orbital	Orbital exponent	H_{ii} (eV)	Reference
Sn	5*s*	2.126	−14.56	13
	5*p*	2.126	−6.84	
Br	4*s*	2.638	−24.00	14
	4*p*	2.257	−12.30	
Fe	4*s*	1.600	−9.91	15, 16
	4*p*	1.600	−5.07	
	3*d*	2.700	−12.63	
C	2*s*	1.625	−21.40	17
	2*p*	1.625	−11.40	
O	2*s*	2.275	−32.30	17
	2*p*	2.275	−14.80	
H	1*s*	1.300	−13.60	17

The total energy of molecule, orbital energies, orbital coefficients, net atomic charges (Table 5), state density, and overlap populations (Table 6) were obtained.

Table 5

Net charges

Sn	2.0855
Br	−0.6274
Fe(1)	0.3685
Fe(2)	0.3786

Table 6

Overlap population

Bond	*ss*	*sp*	*sd*	*ps*	*pp*	*pd*	*ds*	*dp*	*dd*	Summation
Sn–Br	0.0184	0.1214	0.0	0.0310	0.1874	0.0	0.0	0.0	0.0	0.3582
Sn–Fe(1)	0.0309	−0.0319	0.0263	0.0412	−0.0047	0.0559	0.0	0.0	0.0	0.1177
Sn–Fe(2)	0.0297	−0.0341	0.0264	0.0412	−0.0058	0.0567	0.0	0.0	0.0	0.1142
Sn–C(31)	0.1002	0.1713	0.0	0.0543	0.2057	0.0	0.0	0.0	0.0	0.5315
Fe(1)–C(11)	−0.0454	0.0044	0.0	−0.2116	0.0110	0.0	0.0082	0.0600	0.0	−0.1732
Fe(1)–C(12)	−0.0462	−0.0010	0.0	−0.2169	0.0014	0.0	0.0064	0.0467	0.0	−0.2096
Fe(1)–C(13)	−0.0424	0.0013	0.0	−0.2152	0.0028	0.0	0.0063	0.0451	0.0	−0.2020
Fe(1)–C(14)	−0.0462	0.0037	0.0	−0.2212	0.0106	0.0	0.0086	0.0633	0.0	−0.1810
Fe(1)–C(15)	−0.0417	0.0199	0.0	−0.2126	0.0019	0.0	0.0053	0.0391	0.0	−0.1879
Fe(1)–C(111)	0.0479	0.0523	0.0	−0.2042	0.0042	0.0	0.0666	0.2430	0.0	0.2099
Fe(1)–C(112)	0.0399	0.0489	0.0	−0.2087	0.0009	0.0	0.0682	0.2521	0.0	0.2014
Fe(2)–C(21)	−0.0421	0.0015	0.0	−0.2131	0.0029	0.0	0.0062	0.0449	0.0	−0.1995
Fe(2)–C(22)	−0.0454	0.0029	0.0	−0.2154	0.0105	0.0	0.0088	0.0603	0.0	−0.1782
Fe(2)–C(23)	−0.0383	0.0216	0.0	−0.2072	0.0036	0.0	0.0051	0.0398	0.0	−0.1753
Fe(2)–C(24)	−0.0399	0.0096	0.0	−0.2062	0.0102	0.0	0.0076	0.0568	0.0	−0.1617
Fe(2)–C(25)	−0.0420	0.0012	0.0	−0.2101	0.0023	0.0	0.0063	0.0443	0.0	−0.1979
Fe(2)–C(221)	0.0408	0.0494	0.0	−0.2118	−0.0007	0.0	0.0687	0.2480	0.0	0.1945
Fe(2)–C(222)	0.0344	0.0469	0.0	−0.2128	−0.0045	0.0	0.0698	0.2485	0.0	0.1824

Discussion

Description of molecular structure

Figure 1 shows the molecular configuration and atomic labelling, and Fig. 2 shows the molecular packing in a unit cell. The C(31) (*p*-tolyl), the bromine atom, and the two iron atoms are bonded to the central tin atom in a distorted tetrahedral arrangement. Each iron exhibits an approximately octahedral environment with the cyclopentadienyl moiety occupying three coordination sites and the tin and two carbonyls occupying the other three sites. Two different Sn–Fe bond distances, 2.543(1) and 2.536(1) Å, are observed. Bond angles (°) around the tin atom are Fe(1)–Sn–Fe(2) 123.01(2), Br–Sn–Fe(1) 106.09(2), Br–Sn–Fe(2) 103.52(2), Fe(1)–Sn–C(31) 110.6(1), Fe(2)–Sn–C(31) 112.0(1), and Br–Sn–C(31) 98.0(1). The Fe(1)–Sn–Fe(2) angle of 123.01° and the Br–Sn–C(31) angle of 98.0° show a large deviation from tetrahedral geometry.

It is reported that the Sn–Fe bond distance for compounds with the general formula $[\eta\text{-}C_5H_5Fe(CO)_2]_2SnR_2$ changes with the electronegativity of the R groups, for instance, when R_2 are two methyls, the Sn–Fe bond distance is 2.60 Å [4], when R_2 are $C_5H_5Mo(CO)_3$ and chlorine, it is 2.583 Å [7], when R_2 are two ONO groups, it is 2.56 Å [3], and when R_2 are two chlorines, the Sn–Fe bond distance is 2.492 Å [2]. Our title compound has Sn–Fe bond distances of 2.543 and 2.536 Å, which means they lie between those for $\text{-}Sn(CH_3)_2$ and $\text{-}SnCl_2$. The fact that the Sn–Fe distance decreases with an increase in electronegativity of the R groups indicates a transfer of electron density from iron to tin, and this probably involves the transfer of iron 3*d* electrons to the tin *p* orbital vacated by the electron-withdrawing substituents through an inductive effect.

Bonding of the central tin atom

The total number of orbitals is 143 and the number of occupied orbitals is 76. The calculated total electronic energy is −2587.08 eV. The HOMO energy is

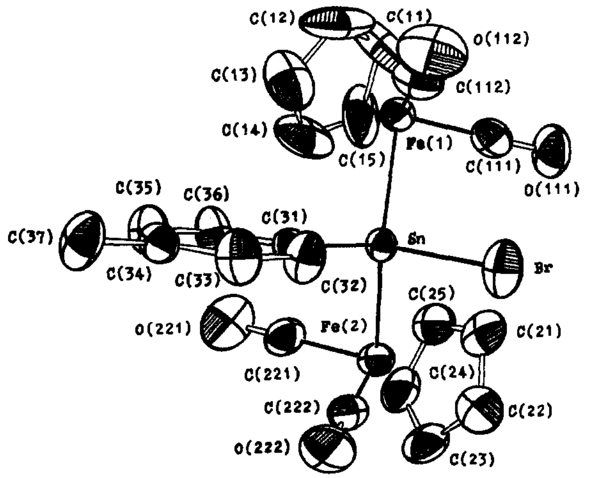

Fig. 1. Molecular structure of $[\eta\text{-}C_5H_5Fe(CO)_2]_2Sn(p\text{-}CH_3C_6H_4)Br$.

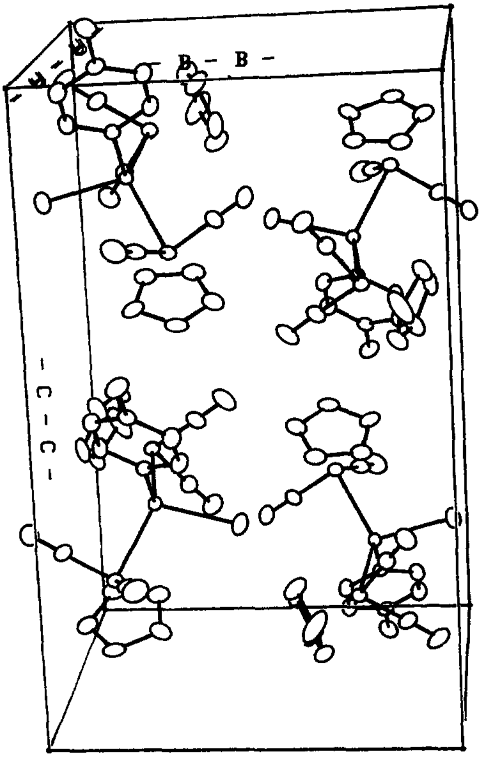

Fig. 2. Packing of molecules in a unit cell.

−11.10 eV and the LUMO energy is −8.85 eV. The difference of energy between HOMO and LUMO is 3.25 eV which accounts for the stability of this compound. The atomic net charges are given in Table 5 and the overlap populations between atoms are given in Table 6.

The bromine and *p*-tolyl groups attached to tin are regarded as electronegative univalent substituents. The metal group, $C_5H_5Fe(CO)_2$, in Sn–Fe bonding is conventionally regarded as the zero-valent substituent. The central tin atom bears a positive charge of 2.0855 corresponding to its formal oxidation state of +2. The Fe atom in $C_5H_5Fe(CO)_2$ has a formal oxidation state of +1, however it only has positive charge of +0.375(av.) because of the electron-donating properties of the attached carbonyls and the delocalized C_5H_5 π-bonding. The overlap population between Sn and Fe is 0.116(av.) due to overlapping of the Sn *p* and Fe *d* orbitals (mainly p_x–$d_{x^2-y^2}$ confirmed by the orbital coefficients) and overlapping of the Sn *p* and Fe *s* orbitals. So, the Sn–Fe bonds are predominantly *s*-character. The overlap populations for Sn–Br and for Sn–C(31) are mainly due to overlapping by the *p* orbitals of these atoms.

Bent [18] described that atomic *s*-character predominates in orbitals directed toward electropositive substituents while *p*-character predominates in orbitals directed toward those which are more electronegative. Here Sn acquires more *p* character in that it is directed toward Br and C(31), which are electronegative. Bent also stated that in the absence of marked steric effects, replacement in the X–A–Y structure of X, by an atom which is more electronegative than X, causes the adjacent A–Y bond to become shorter. This fact is confirmed by the decrease in the Sn–Fe bond distance with the increase in electronegativity of the substituents attached to tin (vide supra). Finally, for compounds of B_2XA_2 type, if A is more electronegative than B, X should induce its *s*-character in those orbitals that are directed toward B, thus the A–X–A angle becomes smaller than, and the B–X–B angle becomes greater than the tetrahedral value of 109°28′. The fact that the Fe(1)–Sn–Fe(2) angle is 123.01° and that of Br–Sn–C(31) is 98.0° agrees well with our calculated result that Sn is bonded to the electropositive Fe(1) and Fe(2), to the electronegative Br and C(31).

Acknowledgement

The authors thank Mr. Lo Xin-Cai and Mr. Li Jing for their assistance with some of the calculations.

References

1 S.V. Dighe and M. Orchin, J. Am. Chem. Soc., 87 (1965) 1146.
2 J.E. O'Connor and E.R. Corey, Inorg. Chem., 6 (1967) 968.
3 B.P. Bir'yukov, Yu.T. Struchkov, K.N. Anisimov, N.E. Kolobava and V.V. Skripkin, Chem. Comm., (1967) 750.
4 B.P. Bir'yukov, Yu.T. Struchkov, K.N. Anisimov, N.E. Kolobava and V.V. Skripkin, Chem. Comm., (1968) 159.
5 B.P. Bir'yukov, Yu.T. Struchkov, K.N. Anisimov, N.E. Kolobava and V.V. Skripkin, Chem. Comm., (1968) 1193.
6 R.F. Bryan, J. Chem. Soc. (A), (1967) 192.
7 J.E. O'Connor and E.R. Corey, J. Am. Chem. Soc., 89 (1967) 3931.
8 P.T. Greene and R.F. Bryan, J. Chem. Soc. (A), (1970) 2261.
9 Hsu-Kun Wang, Xiang-Yang Liu, Zheng-Zhi Zhang and Shu-Sen Liang, Acta Chim. Sinica, in press.
10 A.C.T. North, D.C. Philips and F.S. Mathews, Acta Crystallogr., Sect. A, (1968) 251.
11 B.A. Frenz, in H. Schenk, R. Olthof-Hazelkamp, H. van Koningsveld and G.C. Bassi (Eds.), Computing in Crystallography, Delft University Press, Delft, 1978, pp. 64–71.
12 Xu Yin-Cheng, Wu Yong-Hua, EHMO Program, Dalian Institute of Chemical Physics, Chinese Academy of Science, 1980.
13 J.S. Tse, T.K. Shan and G.M. Bancroft, Can. J. Chem., 57 (1979) 2223.
14 G. Hojer and S. Meza, Acta Chem. Scand., 26 (1972) 3723.
15 L.L. Lohr, Jr. and W.N. Lipscomb, Inorg. Chem., 3 (1964) 22.
16 J.W. Lauher, M. Elian, R.H. Summerville and R. Hoffmann, J. Am. Chem. Soc., 98 (1976) 3224.
17 A.R. Pinhas, T.A. Albright, P. Hofmann and R. Hoffmann, Helv. Chim. Acta, 63 (1980) 29.
18 H.A. Bent, Chem. Rev., 61 (1961) 275.